VOC species and emission inventory from vehicles and their SOA formation potentials estimation in Shanghai, China

C. Huang[1*], H. L. Wang[1], L. Li[1], Q. Wang[1], Q. Lu[1], J. A. de Gouw[2], M. Zhou[1], S. A. Jing[1], J. Lu[1], C. H. Chen[1]

1. State Environmental Protection Key Laboratory of the Formation and Prevention of Urban Air Pollution Complex, Shanghai Academy of Environmental Sciences, Shanghai, China

2. Earth System Research Laboratory, Chemical Sciences Division, NOAA, 325 Broadway, Boulder, Colorado 80305, USA

Abstract: VOC species from vehicle exhaust and gas evaporation were investigated by chassis dynamometer and on-road measurements of 9 gasoline vehicles, 7 diesel vehicles, 5 motorcycles, and 4 gas evaporation samples. The SOA mass yields of gasoline, diesel, motorcycle exhausts, and gas evaporation were estimated based on the mixing ratio of measured C2-C12 VOC species and references IVOC species. High aromatic contents were measured in gasoline exhaust and contributed more SOA yield comparatively. A vehicular emission inventory was compiled based on a local survey of on-road traffic in Shanghai and real-world measurements of vehicle emission factors from previous studies in the cities of China. The inventory-based vehicular OA productions to total CO emissions were compared with the observed ΔOA/ΔCO in the urban atmosphere. The results indicate that vehicles dominate the POA emissions and OA productions, which contributed about 40% and 60% of OA mass in the urban atmosphere of Shanghai. Diesel vehicles, which accounted for less than 20% of VKT, contribute more than 90% of vehicular POA emissions and 80%-90% of OA mass derived by vehicles in urban Shanghai. Gasoline exhaust could be an important source of SOA formation. Tightening the limit of aromatic content in gasoline fuel will be helpful to reduce its SOA contribution. IVOCs in vehicle exhausts have great contributions to SOA formation in the urban atmosphere of China.

* Correspondence to C. Huang (huangc@saes.sh.cn)

However, more experiments need to be conducted to determine the contributions of IVOCs to OA pollution in China.

Key words: SOA; VOC species; vehicle emission; emission inventory; organic aerosol

1. Introduction

Secondary organic aerosol (SOA) accounts for a significant fraction of ambient tropospheric aerosol (Hallquist et al., 2009; Jimenez et al., 2009). De Gouw and Jimenez (2009) suggested that SOA from urban sources may be the dominant source of organic aerosol globally between 30 and 50 latitude.

Gas-phase oxidation of volatile organic compounds (VOCs) has traditionally been considered to be the major source of urban SOA formation. VOCs are oxidized to low vapor pressure reaction products by OH radical, ozone, and NO_3 radical, and eventually form organic aerosol (OA) in the atmosphere. Odum et al. (1997) investigated the SOA formation from vaporized reformulated gasoline and found single light aromatic hydrocarbons are responsible for the majority of SOA formation. Kleindienst et al. (2002) verified that 75–85% of the SOA was due to reaction products of C6-C9 light aromatic compounds from automobile exhaust. Robinson et al. (2007) further recognized that intermediate-volatile organic compounds (IVOCs) and semi-volatile organic compounds (SVOCs) are also important sources for OA production based on the smog chamber studies of diesel exhaust and wood fire (Weitkamp et al., 2007; Grieshop et al., 2009). Their subsequent study pointed IVOCs such as long-chain and branched alkanes from vehicle exhaust play more important roles in SOA production compared with other combustion emissions (Jathar et al., 2013). A recent study from Zhao et al. (2014) concluded that primary IVOCs were estimated to produce about 30% of newly formed SOA in the afternoon during CalNex campaign in Pasadena, California.

Due to the abundance of reactive organic compounds, vehicle emission has been recognized as a major source of urban SOA formation (Stone et al., 2009; Liu et al.,

2012; Borbon et al., 2013). Laboratory chamber studies also report significant SOA production from diesel, gasoline, and motorcycle exhaust photo-oxidation (Hung et al., 2006; Weitkamp et al., 2007; Chirico et al., 2010; Nordin et al., 2013; Platt et al., 2013). Current research is now focusing on the relative importance of gasoline and diesel vehicles to urban SOA formation. Bahreini et al. (2012) and Hayes et al. (2013) suggested gasoline emissions dominate over diesel in urban SOA formation by field studies. Gentner et al. (2012) argued diesel is responsible for 65% to 90% of vehicular-derived SOA based on the estimation of SOA formation from gasoline and diesel fuel compositions.

Shanghai is one of the most urbanized cities in the Yangtze River Delta (YRD) region in China. The YRD region occupies 2% of land area and generates 8%-12% of the primary $PM_{2.5}$ and the emissions of its precursors in China (Huang et al., 2011). Motor vehicles are the fastest growing source of pollution in the megacities of China. The number of vehicles in Shanghai was doubled in the last decade and reached 2.6 million (about 107 units per 1000 capita) in 2012 (SCCTPI, 2013). Gasoline and diesel vehicles increased by 2.8 and 1.3 times, respectively, while motorcycle decreased by 36%. Vehicular emission has been recognized as the largest source of VOCs in urban Shanghai, which contributes 25%~28% of the measured VOC concentrations. Other VOC emission sources were solvent usage, chemical industry, petrochemical industry, and coal burning, etc. (Cai et al., 2010; Wang et al., 2013). Yuan et al. (2013) indicated that VOC emissions are large contributors to SOA formation through field measurements at a receptor site in eastern China. Huang et al. (2012, 2013) reported that 28.7%-32.1% of the fine particle mass is organic matter (OM) and 30.2%-76% of OM is contributed by SOA in the atmosphere of Shanghai and its surrounding areas. Based on the historical measurement data of organic (OC) and element carbon (EC) in $PM_{2.5}$ in the atmosphere in urban Shanghai, the OC/EC ratio shows growing trend from 1999 to 2011, which implies that the secondary fraction of organic matter is playing an increasing role in urban Shanghai (Ye et al.,

2003; Feng et al., 2005; Hou et al., 2011; Cao et al., 2013; Feng et al., 2013). However, the contribution of VOC emissions to SOA formation and the relative importance of vehicular emission remain unclear. At present, vehicle use is experiencing a rapid growth episode in the cities of China. Understanding the contribution of vehicular VOC emissions to SOA formation will be helpful to identify the source of OA and $PM_{2.5}$ pollution in China.

In this study, we first constructed a vehicular emission inventory of Shanghai for the year of 2012. Then the SOA yields of VOCs emissions from different vehicle types were discussed based on the new measurements of VOCs species from a fleet of vehicles in Shanghai. Finally, we calculated the inventory-based vehicular OA production with the ambient observation data to evaluate the OA contribution of vehicle emission. The main purpose of this study is to discuss: (1) the contribution of vehicle emission to OA in urban Shanghai; (2) the relative contributions of gasoline and diesel vehicles to vehicle derived OA.

2. Materials and methods

2.1 Vehicular emission inventory establishment

2.1.1 Methodology of emission inventory compilation

We developed emission inventories for the pollutants including VOCs, CO, EC, and OC with the IVE (International Vehicle Emission) model for Shanghai, China. The methodology of the model has been introduced by Wang et al. (2008). Vehicle kilometers of travel (VKT), vehicle flow distribution, driving pattern, fleet composition and emission factor of each vehicle type were 5 key parameters for the development of vehicle emission inventory. Vehicle emissions can be calculated with Eq. (1).

$$E = \sum_t \left\{ VKT \times f_{[t]} \times EF_{[t]} \times \sum_d \left[f_{[dt]} \times K_{[dt]} \right] \right\} \quad (1)$$

Where, E is emission amount of each vehicle type (g). VKT is Vehicle kilometers of travel of each vehicle type (km). $f_{[t]}$ is the fleet composition of the specific technology

of each vehicle type (%), such as fuel type, engine size, and emission standard. $EF_{[t]}$ is the emission factor of each vehicle technology ($g \cdot km^{-1}$). $f_{[dt]}$ is the fraction of the driving pattern (%). $K_{[dt]}$ is the correction factor of each driving pattern determined by the model (unitless). Evaporative emissions are also calculated with Eq. (1). $EF_{[t]}$ will be evaporative emission factor of each vehicle technology as the evaporative emissions are calculated.

2.1.2 Road traffic data survey

VKTs and their weights on 3 road types (including highway, arterial road, and residential road) were surveyed from transportation for the year of 2012. VKTs on each road type were further separated into 7 vehicle types by the use of video camera surveys. The distributions of each vehicle type were surveyed on various road types with video cameras from March to May. About 4000 valid hours were obtained on 15 roads covering 3 road types. Survey days included weekdays and weekends and each day covered 24 h. The results show that light-duty vehicles (including light-duty cars, light-duty trucks, and taxis) are the major vehicle types on the road, accounting for 56% of the total flows. Heavy-duty vehicles (including heavy-duty bus, heavy-duty truck, and city bus) comprise 19% of the whole VKTs in Shanghai. GPS data were used to determine the driving patterns of various vehicle types. The driving patterns were determined by the average speeds and VSP (Vehicle Specific Power) distributions. We installed GPS units on light-duty cars, taxis, buses, and heavy-duty trucks to record the driving speeds and altitudes second by second. About 150 hours of valid GPS data were collected in this study. The data covered 2831 km of roads and were composed of 3 road types and 4 vehicle types. VSP of each vehicle and road type can be calculated with Eq. (2) introduced by Jimenez (1999).

$$VSP\left(kW \cdot t^{-1}\right) = v \times \left[1.1a + 9.81 \times \left(a \cdot \tan\left(\sin\left(grade\right)\right)\right) + 0.132\right] + 0.000302 \times v^3 \quad (2)$$

Where, v is vehicle speed ($m \cdot s^{-1}$). a is vehicle acceleration ($m \cdot s^{-2}$). $grade$ is vertical rise/slope length. Table 1 shows the daily VKT and average speeds of various vehicle and road types in 2012.

2.1.3 Fleet composition data survey

Fleet composition data were used to separate the VKT of each vehicle type (as shown in Table 1) into the fractions of specific technologies, such as fuel type, engine size, and emission standard. The data were determined by the ratios of the populations of specific technologies in the vehicle information database from the Vehicle Management Department of Public Security Bureau of Shanghai. We call this "static" fleet. Light-duty cars and taxis were mainly composed of gasoline vehicles, which occupied 98% and 97%, respectively. Diesel vehicles dominated in light-duty truck, heavy-duty bus, heavy-duty truck, and city bus, comprising 56%, 91%, 89%, and 98%, respectively. Euro 2 vehicles were the majority of light-duty cars and light-duty trucks, accounting for 51% and 68%, respectively. Heavy-duty buses and trucks were mainly composed of Euro 2 and Euro 3 diesel vehicles, which comprised 40% and 45% of each vehicle type. However, the fraction of each specific technology should be changed with its occurrence frequency in the real-world. Generally, older vehicles show less occurrence frequency than newer vehicles, which means the annual mileage of older vehicle should be less than the newer one. For this reason, we considered to adjust the fleet compositions according to their real-world annual average mileages. About 30,000 vehicles were surveyed at 4 inspection stations in this study. Vehicle age and odometer reading were recorded for each vehicle. The survey data showed that the annual average mileages of light-duty truck, heavy-duty bus, and heavy-duty truck tended to decrease with the increase of their vehicle ages. The "adjusted" fleet compositions were determined by the multiplication of vehicle populations and their surveyed annual mileages. Fig. 1 shows the static and adjusted fraction by each vehicle type in Shanghai. It is indicated that the adjusted fractions of the older vehicles with pre-Euro and Euro 1 emission standard for light-duty truck, heavy-duty bus, heavy-duty truck, and city bus were much lower than those of the static ones. Correspondingly, the adjusted fractions of the newer vehicles with Euro 3 emission standard increased a lot compare with the static ones.

166 2.1.4 Vehicle emission factors

167 The emission factors of each vehicle technology were modeled with the IVE
168 model. However, most of the default emission factors in the model are based on the
169 measurements in the US. To localize the emission factors in this study, we collected
170 the published emission factors based on the real-world measurements in the previous
171 studies to adjust the modeled emission factors. The measurements were all conducted
172 with Portable Emission Measurement Systems (PEMS) under designed driving routes
173 in the cities of China. The cities included Shanghai, Beijing, Guangzhou, Xi'an,
174 Shenzhen, Jinan, and Yichang (Chen et al., 2007; Huo et al., 2012a; Huo et al., 2012b;
175 Wu et al., 2012; Huang et al., 2013). Fig. 2 shows the comparisons of the adjusted
176 emission factors with the measured ones. The evaporative emission factors were not
177 adjusted due to the lack of measurement data. Default factors in the model were used
178 to calculate evaporative emissions in this study. It is indicated that the adjusted
179 emission factors of each vehicle type generally fit well with the measured results. The
180 emission factors are reliable to be used to establish the emission inventory.

181 2.2 VOC species measurements and SOA yield estimation

182 2.2.1 VOC sampling

183 The exhaust from 4 light-duty gasoline vehicles (LDGVs), 5 taxis, 5 heavy-duty
184 diesel trucks (HDDTs), 2 city buses (buses), and 5 motorcycles (MTs) were measured
185 in June 2010. LDGVs, taxis, and MTs were fueled by gasoline. HDDTs and buses
186 were fueled by diesel. The emission standards of the tested vehicles covered Euro 1 to
187 Euro 3 and their model years covered 2001 to 2009. All MTs were 4-stroke with 125
188 cc displacement and without catalytic converter or any other pollution control device.
189 All gasoline vehicles were equipped with catalytic converters. Diesel vehicles didn't
190 install any aftertreatment device like DPF (Diesel Particle Filter). Table 2 lists the
191 detailed information of the tested vehicles. Commercially available fuels were used in
192 the test. The fuel quality met the requirements of the local standard in Shanghai. The
193 sulfur contents of both gasoline and diesel fuel were below 50 ppm.

All the automobiles were measured on chassis dynamometers. LDGVs and taxis were measured utilizing a vehicle mass analysis system (VMAS), which was widely used in in-use vehicle inspection stations in China. VOC sample was collected from a 1-bag test of the Economic Commission of Europe (ECE) urban cycle. The highest speed reaches 50 $km \cdot h^{-1}$ and the average speed is about 18.8 $km \cdot h^{-1}$. HDDTs and buses were measured on a loaded mode test cycle. The tested vehicles were operated on idling and a test cycle which simulates high engine loads under 100%, 90%, and 80% of their maximum powers. The highest speed reaches 70 $km \cdot h^{-1}$. MT exhausts were sampled while operating on the road. A GPS unit was installed on the tested motorcycles to record the speeds second by second. The highest speed reached 50 $km \cdot h^{-1}$ and the average speed was about 20 $km \cdot h^{-1}$. Vehicle exhaust was sampled into a Summa canister (Entech Inst., USA) during the whole driving cycle. We also collected the samples of gasoline vapor at 4 gas stations in Shanghai to analyze the VOC species of non-tailpipe gasoline.

2.2.2 VOC analysis

Concentration of C2-C12 VOCs in samples were determined by a GC–MS system (Agilent 7890A/5975C) with standard gases prepared by Spectra Gas. The samples collected in the Summa canister were pre-concentrated to an acceptable level for the analytical devices using a 7100A pre-concentrator (Entech Inst., USA) with an Entech 7016CA automatic sample injector. A 50 mL sample was extracted by the pre-concentrator into a 1/4 inch liquid nitrogen cold trap to remove water and CO_2, and then separated by GC and detected by MS. The carrier gas was helium.

2.2.3 SOA yield estimation

To investigate the SOA formation potentials of VOC emissions in vehicle exhausts and gas evaporation, we calculated the SOA yields of the exhausts from gasoline, diesel, and motorcycle vehicles and evaporative emissions with the following equation.

$$Y_j = \frac{\sum \left(C_{i,j} \times Y_i\right)}{\sum VOC_j} \quad (3)$$

Where, Y_j is the SOA yield of source j (unitless). $C_{i,j}$ is the weight percent (by carbon) of species i in which can be identified by measurements or references from source j (wtC%). VOC_j is the weight percent (by carbon) of total identified SOA precursors and unidentified species. Identified non-SOA precursors were excluded from total VOC emissions. The weight percentages of identified species were determined by the measurements above. The unidentified species accounted for about 25%, 60%, and 50% in gasoline, diesel, and motorcycle exhausts, repectively. Considering IVOCs which had high SOA formation potentials were not measured in this study, we combined the amounts of alkanes and aromatics larger than C12 and polycyclic aromatics from Gentner et al. (2012) with the identified species to compare the differences of SOA yields with or without IVOCs. Y_i is the yield of species i under high-NOx condition considering the study was focusing on urban area with high NOx concentration (unitless). The yield for each SOA precursor was referenced from Gentner et al. (2012), which listed the yields of known and estimated compounds using a combination of measured SOA yields derived from laboratory-chamber experiments and approximate SOA yields based on box modeling.

2.3 Air pollution observation and vehicular OA contribution determination

2.3.1 Air pollution observation

To estimate the vehicular OA production in the atmosphere, we calculated the SOA formation potentials from vehicular VOC emissions based on observation data with a photochemical- age-based parameterization method. The observation data were obtained from a monitoring site on the roof of a 5-floor building (15 m high above the ground) at Shanghai Academy of Environmental Science (31.17ºN, 121.43ºE), which was located southwest of urban area of Shanghai. The site was mostly surrounded by commercial properties and residential dwellings. Vehicle exhaust was a major source of pollutants near this site. Fig. S1 shows the location of monitoring site in this study.

Carbon monoxide was continuously measured by an ECOTECH EC9820 CO analyzer. $PM_{2.5}$ concentration was measured by a Thermo Fisher commercial instrument β-ray particulate monitor. Organic carbon (OC) and elemental carbon (EC) were measured by a carbon analyzer (model RT-4, Sunset Laboratory Inc.). Water soluble ions were measured by a commercial instrument for online monitoring of aerosols and gases (MARGA, model ADI 2080, Applikon Analytical B.V.). Individual VOC species were continuously measured every 30 minutes by two on-line gas chromatographs with flame ionization detector (GC-FID) systems (Chromato-sud airmoVOC C2–C6 #5250308 and airmoVOC C6–C12 #2260308, France). Fig. S2 shows the time series data of meteorological parameters and concentrations of major air pollutants observed in urban Shanghai in summer (August in 2013) and winter (January in 2013). We didn't measure the OA concentration due to the lack of observation equipment. The OA concentrations were determined by OC concentrations multiplying the OM/OC ratio. Turpin et al. (2001) suggested a ratio around 1.2-1.6 from fresh emission to aged air mass in remote area. Considering our study was mainly focusing on urban area where emissions were not fully aged, we used the ratio of 1.4 to convert OC concentrations.

2.3.2 OA production estimation

The evolution of primary VOC emissions to SOA formation is determined by OH exposure in the atmosphere. The OH exposure can be calculated with Eq. (4) developed by de Gouw et al. (2005, 2008).

$$\Delta t \cdot [OH] = \frac{1}{(k_X - k_E)} \times \left[\ln\left(\frac{[X]}{[E]}\Big|_{t=0} \right) - \ln\left(\frac{[X]}{[E]} \right) \right] \quad (4)$$

Here, Δt is photochemical age (h). $[OH]$ is the average OH radical concentrations (molecules·cm^{-3}). The ratio of m,p-xylene to ethylbenzene (X/E) was considered as a photochemical clock. k_X and k_E are the OH rate constants of m,p-xylene (18.9×10^{-12} cm^3·molecule^{-1}·s^{-1}) and ethylbenzene (7.0×10^{-12} cm^3·molecule^{-1}·s^{-1}) (Yuan et al., 2013). $[X]/[E]|_{t=0}$ and $[X]/[E]$ are initial emission ratio and the ratio after

photochemical reaction of m,p-xylene to ethylbenzene. The concentrations of m,p-xylene and ethylbenzene showed good correlations during the observation (Fig. S3). The different diurnal variations of m,p-xylene and ethylbenzene indicated that they are engaged in different chemical reactions in the daytime (Fig. S4). Fig. 3 illustrates the diurnal distributions of the ratios of observed m,p-xylene to ethylbenzene in summer and winter of 2013. The initial emission ratios of m,p-xylene to ethylbenzene were determined by the X/E ratio on 97.5 percentiles, which were 2.17 and 1.68 in summer and winter, respectively.

OA production is determined by the loss terms and formation rates of OA concentration after POA emissions exhaust into the atmosphere. de Gouw et al. (2008) introduced a method to explain the OA evolution during photochemical aging of urban plumes as shown by Eq. (5).

$$\frac{\Delta OA}{\Delta CO} = \frac{\Delta POA}{\Delta CO} + \frac{\Delta SOA}{\Delta CO} = ER_{POA} \times \exp\left(-L_{OA} \cdot \Delta t\right) + ER_{VOC_j} \times Y_j \times \frac{P_{OA}}{L_{OA} - P_{OA}} \times \left[\exp\left(-P_{OA} \cdot \Delta t\right) - \exp\left(-L_{OA} \cdot \Delta t\right)\right] \quad (5)$$

Here, $\Delta OA/\Delta CO$ is the ratio of OA formation versus CO emission after photochemical reaction ($\mu g \cdot m^{-3} \cdot ppmv^{-1}$). ER_{POA} is the primary emission ratio of OA to CO emission ($\mu g \cdot m^{-3} \cdot ppmv^{-1}$). ER_{VOCj} is the primary emission ratios of VOC (including SOA precursors and unidentified species) from source j to CO emission in the unit of $ppbv^{-1} \cdot ppmv^{-1}$. Y_j is the SOA yield of source j, which is determined by Eq. (3). L_{OA} and P_{OA} are the loss and formation rate of organic aerosol, respectively. We used the empirical parameters derived by de Gouw et al. (2008), which were 0.00677 h^{-1} and 0.0384 h^{-1}, respectively. Δt is the photochemical age calculated by equation (4). Because there is no OH measurement in Shanghai, we reference the 24-h average OH concentration (3×10^6 molecules$\cdot cm^{-3}$) from de Gouw et al. (2008).

2.3.3 Determination of vehicular OA contribution

The observed ΔOA/ΔCO in the atmosphere represents the ratio of total POA emissions and their SOA formation to total CO emissions from all sources, which can be explained by Eq. (6) as follows.

$$\left(\frac{\Delta OA}{\Delta CO}\right)_{obs} = \frac{POA_{total} + SOA_{total}}{CO_{total}} = \frac{\left(POA_{veh} + SOA_{veh}\right)}{CO_{total}} + \frac{\left(POA_{oth} + SOA_{oth}\right)}{CO_{total}} = \frac{OA_{veh}}{CO_{total}} + \frac{OA_{oth}}{CO_{total}} \quad (6)$$

The contribution of vehicular OA to total OA production in the atmosphere can be determined by the ratio of OA_{veh}/CO_{total} to $(\Delta OA/\Delta CO)_{obs}$. Here, $(\Delta OA/\Delta CO)_{obs}$ is the ratio of observed ΔOA (Obs, $OA\text{-}OA_{background}$) to observed ΔCO (Obs, $CO\text{-}CO_{background}$) in the unit of $\mu g \cdot m^{-3} \cdot ppmv^{-1}$. OA_{veh}/CO_{total} is the ratio of vehicular POA emission and SOA formation to total CO emissions, which can be calculated by Eq. (5). ER_{POA} and ER_{VOCj} in Eq. (5) should be substituted by the ratios of vehicular POA and VOC emissions to total CO emissions from vehicle and other sources. The total amount of CO emission was 1.2×10^6 tons according to the annually updated emission inventory in Shanghai for the year of 2012. Iron & steel manufacturing was the major source of CO emission, which accounted for 54% of the total. The sector produced 19.7×10^6 and 18×10^6 tons of pig irons and crude steels, and consumed more than 10×10^6 tons of coal in 2012. Vehicles were the second largest source, accounting for 27.8% of the total. Detailed information is shown in Fig. S5. However, considering the observation site was located in the urban area and most of the large CO emission sources were located at the surrounding areas (about 30-50 km from city center), it would be more reasonable to exclude the emissions out of the urban area. The emissions of various sources in the urban area were extracted based on their spatial distributions. Vehicle POA, VOC (including evaporative emissions), and CO emissions in urban area were 1.8, 13.4, and 170.7 k tons, respectively. Vehicles dominated CO emission in urban Shanghai, accounting for 85% of total CO emission in the urban area.

3. Results and discussion

3.1 Vehicle emission inventory

The emissions of CO, NOx, VOCs, EVA (gas evaporation), EC, and POA (OC*1.2) from vehicles were 343.9, 110.9, 39.4, 8.9, 4.0, and 4.3 k tons in Shanghai for the year of 2012 (See Table 3). Gasoline vehicles (including LDGV, Taxi, HDGV,

and Motorcycle) were the major sources of CO, VOCs, and EVA emissions, accounting for 91%, 69%, and 100%, respectively. Diesel vehicles (including LDDV, HDDV, and Bus) were the major source of NOx, EC, and POA emissions, comprising 82%, 99%, and 96%, respectively. CO and VOC (including EVA) emissions decreased by 40% and 38% compared with the results for the year of 2004 from Wang et al. (2008). NOx emission increased by 21%. PM emission were low estimated in that article since the PM emission factors were much lower than real-world measurement data as shown in Fig. 2. Gasoline vehicle emissions have been well controlled even though their VKTs were nearly doubled in the past few years. In comparison, the control effect of diesel vehicle emission was relatively poor. It is clear that diesel exhausts dominate the primary PM (including EC and OA) emissions in Shanghai. However, since VOC emissions are mainly from gasoline vehicles, we will further discuss the contributions of gasoline and diesel exhausts to SOA.

3.2 VOC species of vehicle emissions and gas evaporation

Fig. 4 compares the VOC compositions of the exhausts from different vehicle types and gas evaporation in this study to the results from other countries or regions. Since the VOC species measured in different studies are not the same, we normalized the concentrations of the common species including C2-C12 alkanes, alkenes, alkynes, and single-ring aromatics in each study as 100%. Other compounds and unidentified VOCs were excluded in the comparison.

The weighted percentages of individual VOC for the exhausts from different vehicle types and gas evaporation were listed in Table S1.

The exhausts from gasoline vehicles (including LDGVs and taxis) had similar VOC compositions. Single-ring aromatics were the major species of the exhausts from gasoline vehicles, accounting for 50% of the total VOCs approximately. Straight-chain alkanes, branched alkanes, and cycloalkanes comprised 17.0%, 18.1%, and 6.1% of the total VOCs, respectively. Toluene, m,p-xylene, o-xylene, and ethylbenzene were the main compounds in LDGV and taxi exhausts, accounting for

7.54%, 6.71%, 5.20%, and 4.42% of the total VOCs, respectively. Motorcycle emitted more branched alkanes and less single-ring aromatics than LDGVs and taxis. 2-methylhexane (23.43%) was the most abundant VOC in motorcycle exhausts, followed by m,p-xylene (9.34%), ethylbenzene (5.53%) and o-xylene (4.37%). It was indicated from Fig. 3 that the proportion of single-ring aromatics in LDGV exhausts were higher and the proportion of alkene were lower in this and previous studies in China (Liu et al., 2008; Wang et al., 2013) than those in Hong Kong (Guo et al., 2011) and US (Schauer et al., 2002; Gentner et al., 2013; May et al., 2014). The differences of aromatic content in gasoline fuel in different regions and countries could be the main reason of the difference in the proportion of aromatic compounds in LDGV exhausts. The limit of aromatic content in current gasoline standard in China was 40 vol%, which was much higher than the limits of gasoline standards of the US (22-25 vol%) and Europe (35 vol%).

High proportion of straight-chain alkanes were measured in the exhausts from diesel vehicles, which accounted for 34.9% and 35.6% of the total VOCs from HDDT and bus exhausts, respectively. N-dodecane, propene, n-undecane, acetone, and n-decane were major species in diesel exhausts, accounting for 13.65%, 10.85%, 8.69%, 7.00%, and 6.86% of the total VOCs, respectively. The proportions of straight-chain alkanes in diesel exhausts in this study were much higher than those in the previous studies of the US (Schauer et al., 1999; May et al., 2014). Incomplete combustion of diesel fuel caused by poor engine maintenance could be the main reason for the high straight-chain alkane emissions.

High proportion of alkenes was measured in gas evaporation in this study, which accounted for 40% of the total VOCs. Propane, isopentane, isobutene, 1-pentene, and n-butane were major species in gas evaporation emissions, accounting for 15.99%, 11.87%, 9.69%, 8.87%, and 6.51% of the total VOCs, respectively. The proportions of VOC species in gas evaporation in this study was close to the results in the other study of China (Zhang et al., 2013), but different from the studies in the US (Harley et

al., 2000) and Korea (Na et al., 2004), which reported less alkenes and more branched alkanes in gas evaporation.

3.3 SOA yields of different vehicle exhausts and gas evaporation

VOC species of vehicle emissions and gas evaporation were classified into 5 categories by their chemical classes, and their distributions of carbon numbers were shown in Fig. 5(a). Previous studies have confirmed that IVOCs, which were not detected in this study, played important roles to SOA production (Jathar et al., 2013; Zhao et al., 2014). For this reason, we combined the amounts of S/IVOCs including alkanes and aromatic larger than C12 and polycyclic aromatics in unburned fuels introduced by Gentner et al. (2012). The SOA yields of each vehicle exhaust and evaporative emission were calculated in two scenarios of with (Y2) or without S/IVOCs (Y1) in Fig. 5. The carbon numbers of VOCs in gasoline and motorcycle exhausts mainly concentrated in the intervals between C6 to C9 whether the IVOCs were merged or not. Comparatively, exhausts from diesel vehicles had a wider distribution of carbon number, ranging from C2 to C25. More than half of the species were S/IVOCs and most of them were alkanes. The carbon numbers of VOCs in gas evaporation were mainly distributed within the range of C3-C7, which were much smaller than those in vehicle exhausts.

Fig. 5(b) and (c) show the SOA mass yields and the contributions of different chemical class calculate by measured and combined species, respectively. S/IVOC species had no effect on the SOA yields of gasoline exhausts and evaporative emissions. Aromatics dominated the yields which accounted for almost 100% of the total. However, the SOA yield of diesel exhaust was significantly affected by S/IVOCs. The yield increased from 0.008 to 0.164 when S/IVOCs were considered. Aromatics were still the largest contributors (34.1%) to but not dominating the yield. Next were branched alkanes, polycyclic aromatics, and straight-chain alkanes, which accounted for 24.9%, 17.8%, and 12.8%.

The SOA yield of gasoline exhaust was larger than the yield of liquid gasoline

reported by Gentner et al. (2012). We found the aromatic contents in gasoline exhausts of this study which dominated the SOA yield were much higher than those in the reference. This may be due to the loose limit of aromatics for the gasoline fuel in China. However, the estimated yield of gasoline exhaust was much lower than the effective yields (3-30%) of LEV-1 (tier 1 of low emission vehicle standard in California, US) gasoline vehicles (similar to Euro 1-3 LDGVs tested in this study) investigated using a smog-chamber experiment by Gordon et al. (2014a). The reason for the underestimate was still unclear. In contrast, the estimated SOA yield of diesel exhaust which combined S/IVOCs (Y2) was higher than the average effective yields (9±6%) for HDDVs without DPF based on smog-chamber experiments by Gordon et al. (2014b). Since there were few experiments on motorcycle exhaust, we compared the SOA yield of motorcycle exhaust with the experiment results from the exhausts of 2- and 4-stroke gasoline off-road engines (Gordon et al., 2013). Neither motorcycles nor off-road engines had catalytic converter. The estimated yield was close to the experiment results of off-road engine exhausts (2-4%).

3.4 Primary emission ratio and SOA formation potential based on observation

Fig. 7 is a scatterplot of OA versus CO concentrations measured in urban Shanghai in the summer and the winter of 2013. The observation data were color-coded by OH exposure ($\Delta t \cdot [OH]$) determined by equation (4). It was indicated from the figure that the ratios of OA to CO concentrations generally showed growing trends with the increase of OH exposure both in summer and winter. The results were similar to the previous studies in the United States, Japan, and Mexico (Bahreini et al., 2012; de Gouw et al., 2008; Takegawa et al., 2006; DeCarlo et al., 2008). The primary emission ratios of POA to CO were determined by the minimum slopes of the observed OA to CO concentrations, about 12 $\mu g \cdot m^{-3} \cdot ppmv^{-1}$ in both summer and winter (as shown by the dotted grey lines). The maximum slopes of OA to CO were 50 and 35 $\mu g \cdot m^{-3} \cdot ppmv^{-1}$ (as shown by the dotted black lines) in summer and winter,

441 respectively. The SOA formation ratio in summer was much higher than in winter.
442 The inventory-based vehicular POA emission to total CO emission was 11.6
443 $\mu g \cdot m^{-3} \cdot ppmv^{-1}$ in the urban area of Shanghai (shown by the dotted yellow lines),
444 almost the same with primary emission ratio observed in the atmosphere, which
445 indicated that vehicles dominated the POA emissions in urban Shanghai. The dotted
446 orange line in Fig. 6 represents the maximum OA production ratio (assuming SOA
447 precursors were 100% reacted) calculated with the SOA yields in Y2 scenario. The
448 maximum OA production ratio reached 18.7 $\mu g \cdot m^{-3} \cdot ppmv^{-1}$. It was considerable
449 underestimated compared with the observation data, which implied that the SOA
450 yields derived by known and estimated species were still far from explaining the
451 actual SOA formation rate in the atmosphere. For this reason, we introduced the
452 measured SOA yield of gasoline exhaust (~0.190) from Gordon et al. (2014a) to
453 substitute the yield for gasoline vehicles (0,039) in Y2 scenario and defined the new
454 group as Y3 scenario. The maximum OA production ratio (shown by the dotted red
455 lines) increased to 27.3 $\mu g \cdot m^{-3} \cdot ppmv^{-1}$, but still failed to reach the max. observed
456 $\Delta OA/\Delta CO$. There must be other emission sources of SOA precursors in the
457 atmosphere of Shanghai. Previous studies have revealed that VOC emissions from
458 solvent usage, chemical and petrochemical industrial, and coal burning, etc.
459 comprised more than 70% of the observed VOCs in the atmosphere of urban Shanghai
460 (Cai et al., 2010; Wang et al., 2013). The SOA productions of VOC emissions from
461 these sources also cannot be ignored.

462 3.5 Estimation of vehicular OA contribution in the urban atmosphere

463 Fig. 7 shows the diurnal variations of average observed $\Delta OA/\Delta CO$ and OH
464 exposure in summer and winter. There was a strong correlation between the observed
465 $\Delta OA/\Delta CO$ and OH exposure, which indicated the photooxidation dominated the SOA
466 formation in the atmosphere. In the role of photochemical reaction, the observed
467 $\Delta OA/\Delta CO$ showed rapid growth trend in the afternoon in summer and reached a peak
468 around 13:00~14:00. The average observed $\Delta OA/\Delta CO$ in urban atmosphere of

Shanghai were 33.2 and 21.1μg·m^{-3}·ppmv^{-1} in summer and winter, respectively.

To evaluate the contribution of vehicle emission to OA production in urban atmosphere, we estimated the vehicular OA formation ratio to total CO emissions with Eq. (5) in two scenarios. Fig. 7(a) and (b) show the results in Y2 scenario. The SOA yields of gasoline, diesel, and motorcycle exhausts and gas evaporation were 0.039, 0.164, 0.021, and 0.0007, respectively. Fig. 7(c) and (d) show the results in Y3 scenario. The SOA yield of gasoline exhaust was replaced to 0.190 based on the experiment results (Gordon et al., 2014a). The photochemical age (Δt) in each hour was calculated with Eq. (4). Due to the lack of OH measurement in Shanghai, we referenced the 24-h average OH concentration (3×10^6 molecules·cm^{-3}) from de Gouw et al. (2008). The grey and yellow lines were the ratio of vehicular POA and OA production to total CO emissions. The average vehicular OA production ratios to total CO emission in the urban area were 12.5 μg·m^{-3}·ppmv^{-1} and 12.2 μg·m^{-3}·ppmv^{-1} in summer and winter in Y2 scenario, and 14.0 μg·m^{-3}·ppmv^{-1} and 13.2 μg·m^{-3}·ppmv^{-1} in Y3 scenario. The vehicular OA mass accounted for 39% and 58% of the average observed OA in summer and winter in the urban atmosphere of Shanghai in Y2 scenario. The contributions would increase to 43% and 63% in Y3 scenario. It was indicated that vehicle emission was the major source of OA mass in the urban atmosphere of Shanghai. Enhancing the SOA yield of gasoline exhaust increased about 4%-5% of their contributions to OA, which implied gasoline exhaust didn't dominate the OA mass in the urban atmosphere. Vehicular SOA formation ratios accounted for 7%-10% of the total vehicular OA in Y2 scenario and 14%-20% in Y3 scenario. The SOA formation ratios in both scenarios were lower than expected. There must be other emission sources with high SOA formation potentials in addition to vehicles in the urban atmosphere. The non-fossil VOC emissions from solvent use, chemical and petrochemical industrials, etc. reported by the previous studies could be the rest of contributors (Cai et al., 2010; Wang et al., 2013). Another possible reason was the SOA yields were still underestimated in this study. There were about 30%,

50% and 15% of VOC species still unidentified in gasoline, diesel, and motorcycle exhausts even after we combined the S/IVOC species reported in Gentner et al. (2012). The SOA formation potentials of the identified VOC species may contribute more SOA than expected.

At present, few SOA observations in the cities of China can be referenced to verify the results in this study. Huang et al. (2014) has reported the fossil OA dominated the OA mass (~40%) in Shanghai based on the observation data in the first quarter of 2013, which was slightly lower than our result. The possible reason for the difference could be the location of observation site (close to urban or suburban). However, the studies both indicated that vehicle emission was the major source of OA mass in large cities of China.

3.6 SOA formation contributions of different vehicle types

Fig. 9(a) and (b) show the changes of OA formation ratios in different fuel and vehicle types in Y2 scenario with the increase of the photochemical age. The OA produced from evaporative emissions were combined in gasoline vehicles and corresponding vehicle types. Diesel exhausts dominated the OA productions, which accounted for 96%, 93% and 88% after 0, 6, and 24 hours of photochemical reaction. HDDV and bus were major sources of OA productions. Fig. 9(c) and (d) show the changes of OA formation ratios in Y3 scenario. The contribution of gasoline vehicles in this scenario increased a lot. Although gasoline vehicles only accounted for 4% of POA emission, their contributions to vehicular OA formation increased to 19% and 35% after 6 and 24 hours of photochemical reaction, respectively. LDGV would be the second large contributor after HDDV. It can be indicated that diesel vehicles were the largest contributors to vehicle derived OA in both scenarios although they only accounted for less than 20% of VKTs in Shanghai. Control of the POA emissions and SOA precursors from diesel vehicles are equally important. Gasoline vehicle could be another important contributor to vehicular OA formation. However, there still exist some debates on the SOA yield of gasoline exhaust. It will be meaningful to find out

525 their actual SOA yield and key precursors for urban OA pollution control.

526 **4. Conclusions**

527 To evaluate the OA contribution of vehicle emissions in the urban atmosphere of
528 Shanghai, we developed a vehicular emission inventory and estimated the SOA yields
529 of gasoline, diesel, and motorcycle exhausts and gas evaporation based on measured
530 C2-C12 VOC species and referenced S/IVOC species from Gentner et al. (2012).
531 Higher contents of aromatic were measured in this study and other studies in China
532 compared with the results from the US and European. Loose limit to aromatic
533 contents in the standard of gasoline fuel in China should be responsible for the high
534 aromatic contents, which resulted in larger SOA yield of gasoline exhaust than the
535 results reported by Gentner et al. (2012) based on the same method. However, the
536 estimated yield was still much lower than the results from smog-chamber experiments
537 (Gordon et al., 2014a), which implied the unidentified species were considerable to
538 SOA formation.

539 Vehicles dominated the POA emissions and OA productions in the urban
540 atmosphere of Shanghai. Their contributions to OA productions were about 40% and
541 60% in summer and winter, respectively. The rest of the contributors could be the
542 non-fossil VOC emissions from solvent use, chemical and petrochemical industrials,
543 etc. and the underestimated SOA productions from unidentified VOC or IVOC
544 species in the exhausts. At present, vehicles are experiencing rapid growth trends in
545 the cities of China. Primary emissions and secondary formation of OA derived from
546 vehicles will lead to further deterioration of fine particle pollution in the urban area.
547 Reduction of primary PM emissions and SOA precursors from vehicle exhausts will
548 be helpful to improve the air quality in the cities of China. The results also indicate
549 diesel exhausts dominate the POA emissions in the urban area. Therefore,
550 strengthening the primary PM emission control of diesel vehicles, especially for the
551 older diesel vehicles with loose emission standards as shown by Fig. 2, plays an
552 important role in OA pollution prevention. Now China is conducting the large-scale

elimination of “yellow-labeled” diesel vehicles whose emission standards were lower than Euro 3. It can be expected to effectively reduce the OA pollution caused by diesel vehicles. On the other hand, gasoline exhausts have high potential impacts on SOA formation in the urban area. Tightening the limit of aromatic contents in gasoline fuel will be meaningful to reduce the SOA contributions of gasoline vehicles.

There are still some uncertainties need to be improved in the future. First is the SOA mass yield. More experiments on SOA yields of vehicle exhausts in China will be helpful to the SOA formation potentials of different vehicle types. Especially for gasoline exhausts, the estimated SOA yield was much lower than the experiment results in the US. Vehicular OA contributions will increase about 4%-5% if we replace the estimated SOA yield of gasoline exhaust to the experiment result. It will be meaningful to find out their actual SOA yield and key precursors for urban OA pollution control. Emission inventory is another important source of uncertainty in this study. To reduce the uncertainty of vehicular emission inventory, we localized the vehicle mileage and emission factor data based on the traffic surveys in Shanghai and real-world measurements in some cities of China. However, the CO emission inventories of other sources shown in Fig. S5 still have large uncertainties according to the previous study (Huang et al., 2011). More accurate emission inventory will be helpful to reduce the uncertainty of vehicular OA contribution in this study. However, it can be concluded that vehicle emissions are the most important contributors to OA pollution in the cities of China. Another implication is the potential roles of IVOCs in vehicle exhausts are very important on the SOA formation in the urban area. Therefore, further studies need to pay more attentions to determine the contributions of IVOC emissions to OA pollution in China.

Acknowledgement

This study was supported by the National Key Technology R&D Program via grant No. 2014BAC22B03, the National Natural Science Foundation of China (NSFC) via grant No. 41205122, the Science and Technology Commission of Shanghai

Municipality Fund Project via grant No. 14DZ1202905, and the Shanghai Natural Science Foundation via grant No. 15ZR1434700.

References

Bahreini, R., Middlebrook, A. M., de Gouw, J. A., Warneke, C., Trainer, M., Brock, C. A., Stark, H., Brown, S. S., Dube, W. P., Gilman, J. B., Hall, K., Holloway, J. S., Kuster, W. C., Perring, A. E., Prévôt, A. S. H., Schwarz, J. P., Spackman, J. R., Szidat, S., Wagner, N. L., Weber, R. J., Zotter, P., and Parrish, D. D.: Gasoline emissions dominate over diesel in formation of secondary organic aerosol mass, Geophys. Res. Lett., 39, L06805, doi:10.1029/2011GL050718, 2012.

Borbon, A., Gilman, J. B., Kuster, W. C., Grand, N., Chevaillier, S., Colomb, A., Dolgorouky, C., Gros, V., Lopez, M., Sarda-Esteve, R., Holloway, J., Stutz, J., Petetin, H., McKeen, S., Beekmann, M., Warneke, C., Parrish, D. D., and de Gouw, J. A.: Emission ratios of anthropogenic volatile organic compounds in northern mid-latitude megacities: Observations versus emission inventories in Los Angeles and Paris, J. Geophys. Res.-Atmos., 118, 2041–2057, doi:10.1002/jgrd.50059, 2013

Cai, C. J., Geng, F. H., Tie, X. X., Yu, Q., An, J. L.: Characteristics and source apportionment of VOCs measured in Shanghai, China, Atmospheric Environment, 44, 5005–5014, 2010.

Cao, J. J., Zhu, C. S., Tie, X. X., Geng, F. H., Xu, H. M., Ho, S. S. H., Wang, G. H., Han, Y. M., Ho., K.F.: Characteristics and sources of carbonaceous aerosols from Shanghai, China. Atmos. Chem. Phys., 13, 803–817, 2013.

Chan, A. W. H., Kautzman, K. E., Chhabra, P. S., Surratt, J. D., Chan, M. N., Crounse, J. D., Kürten, A., Wennberg, P. O., Flagan, R. C., and Seinfeld, J. H.: Secondary organic aerosol formation from photooxidation of naphthalene and alkylnaphthalenes: implications for oxidation of intermediate volatility organic compounds (IVOCs), Atmos. Chem. Phys., 9, 3049–3060, doi:10.5194/acp-9-3049-2009, 2009.

Chen, C. H., Huang, C., Jing, Q. G., Wang, H. K., Pan, H. S., Li, L., Zhao, J., Dai, Y., Huang, H. Y., Schipper, L., Streets, D. G.: On-road emission characteristics of heavy-duty diesel

609 vehicles in Shanghai, Atmospheric Environment, 41, 5334-5344, 2007.
610 Chirico, R., DeCarlo, P. F., Heringa, M. F., Tritscher, T., Richter, R., Prévôt, A. S. H.,
611 Dommen, J., Weingartner, E., Wehrle, G., Gysel, M., Laborde, M., and Baltensperger, U.:
612 Impact of aftertreatment devices on primary emissions and secondary organic aerosol
613 formation potential from in-use diesel vehicles: results from smog chamber experiments,
614 Atmos. Chem. Phys., 10, 11545–11563, doi:10.5194/acp-10-11545-2010, 2010.
615 DeCarlo, P. F., Dunlea, E. J., Kimme, J. R., Aiken, A. C., Sueper, D., Crounse, J., Wennberg, P.
616 O., Emmons, L., Shinozuka, Y., Clarke, A., Zhou, J., Tomlinson, J., Collins, D. R.,
617 Knapp, D., Weinheimer, A. J., Montzka, D. D., Campos, T., Jimenez, J. L.: Fast airborne
618 aerosol size and chemistry measurements above Mexico City and Central Mexico during
619 the MILAGRO campaign, Atmos. Chem. Phys., 8, 4027–4048, 2008.
620 de Gouw, J. A., Middlebrook, A. M., Warneke, C., Goldan, P. D., Kuster, W. C., Roberts, J. M.,
621 Fehsenfeld, F. C., Worsnop, D. R., Canagaratna, M. R., Pszenny, A. A. P., Keene, W. C.,
622 Marchewka, M., Bertman, S. B., and Bates, T. S.: Budget of organic carbon in a polluted
623 atmosphere: Results from the New England Air Quality Study in 2002, J. Geophys.
624 Res.-Atmos., 110, D16305, doi:10.1029/2004jd005623, 2005.
625 de Gouw, J. A., Brock, C. A., Atlas, E. L., Bates, T. S., Fehsenfeld, F. C., Goldan, P. D.,
626 Holloway, J. S., Kuster, W. C., Lerner, B. M., Matthew, B. M., Middlebrook, A. M.,
627 Onasch, T. B., Peltier, R. E., Quinn, P. K., Senff, C. J., Stohl, A., Sullivan, A. P., Trainer,
628 M., Warneke, C., Weber, R. J., and Williams, E. J.: Sources of particulate matter in the
629 northeastern United States in summer: 1. Direct emissions and secondary formation of
630 organic matter in urban plumes, J. Geophys. Res.-Atmos., 113, D08301,
631 doi:08310.01029/02007JD009243, 2008.
632 de Gouw, J. and Jimenez, J. L.: Organic Aerosols in the Earth's Atmosphere, Environ. Sci.
633 Technol., 43, 7614–7618, 2009.
634 Feng, J. L., Chan, C. K., Fang, M., Hu, M., He, L. Y., Tang, X. Y.: Characteristics of organic
635 matter in $PM_{2.5}$ in Shanghai, Chemosphere, 64, 1393-1400, 2005.
636 Feng, J. L., Li, M., Zhang, P., Gong, S. Y., Zhong, M., Wu, M. H., Zheng, M., Chen, C. H.,

637 Wang, H. L., Lou, S. R.: Investigation of the sources and seasonal variations of
638 secondary organic aerosols in $PM_{2.5}$ in Shanghai with organic tracers, Atmospheric
639 Environment, 79, 614-622, 2013.
640 Feng, Y. L., Chen, Y. J., Guo, H., Zhi, G. R., Xiong, S. C., Li, J., Sheng, G. Y., Fu, J. M.:
641 Characteristics of organic and elemental carbon in $PM_{2.5}$ samples in Shanghai, China,
642 Atmospheric Research, 92, 434-442, 2009.
643 Gentner, D. R., Isaacman, G., Worton, D. R., Chan, A. W. H., Dallmann, T. R., Davis, L., Liu,
644 S., Day, D. A., Russell, L. M., Wilson, K. R., Weber, R., Uha, A., Harley, R. A., and
645 Goldstein, A. H.: Elucidating secondary organic aerosol from diesel and gasoline
646 vehicles through detailed characterization of organic carbon emissions, P. Natl. Acad. Sci.
647 USA, 109, 18318–18323, 2012.
648 Gentner, D. R., Worton, D. R., Isaacman, G., Davis, L. C., Dallmann, T. R., Wood, E. C.,
649 Herndon, S. C., Goldstein, A. H., Harley, R. A.: Chemical composition of gas-phase
650 organic carbon emissions from motor vehicles and implications for ozone production,
651 Environ. Sci. Technol., 47, 11837−11848, 2013.
652 Gordon, T. D., Tkacik, D. S., Presto, A. A., Zhang, M., Jathar, S. H., Nguyen, N. T., Massetti,
653 J., Truong, T., Cicero-Fernandez, P., Maddox, C., Rieger, P., Chattopadhyay, S.,
654 Maldonado, H., Maricq, M. M., Robinson, A. L.: Primary gas- and particle-phase
655 emissions and secondary organic aerosol production from gasoline and diesel off-road
656 engines, Environ. Sci. Technol., 47, 14137−14146, 2013.
657 Gordon, T. D., Presto, A. A., May, A. A., Nguyen, N. T., Lipsky, E. M., Donahue, N. M.,
658 Gutierrez, A., Zhang, M., Maddox, C., Rieger, P., Chattopadhyay, S., Maldonado, H.,
659 Maricq, M. M., Robinson, A. L.: Secondary organic aerosol formation exceeds primary
660 particulate matter emissions for light-duty gasoline vehicles, Atmos. Chem. Phys., 14,
661 4661–4678, 2014a.
662 Gordon, T. D., Presto, A. A., Nguyen, N. T., Robertson, W. H., Na, K., Sahay, K. N., Zhang,
663 M., Maddox, C., Chattopadhyay, S., Maldonado, H., Maricq, M. M., Robinson, A. L.:
664 Secondary organic aerosol production from diesel vehicle exhaust: impact of

665 aftertreatment, fuel chemistry and driving cycle, Atmos. Chem. Phys., 14, 4643–4659,
666 2014b.
667 Grieshop, A. P., Donahue, N. M., and Robinson, A. L.: Laboratory investigation of
668 photochemical oxidation of organic aerosol from wood fires 2: analysis of aerosol mass
669 spectrometer data, Atmos. Chem. Phys., 9, 2227–2240, 2009.
670 Guo, H., Zou, S. C., Tsai, W. Y., Chan, L. Y., Blake, D. R.: Emission characteristics of
671 nonmethane hydrocarbons from private cars and taxis at different driving speeds in Hong
672 Kong, Atmospheric Environment, 45, 2711–2721, 2011.
673 Hallquist, M., Wenger, J. C., Baltensperger, U., Rudich, Y., Simpson, D., Claeys, M.,
674 Dommen, J., Donahue, N. M., George, C., Goldstein, A. H., Hamilton, J. F., Herrmann,
675 H., Hoffmann, T., Iinuma, Y., Jang, M., Jenkin, M. E., Jimenez, J. L., Kiendler-Scharr, A.,
676 Maenhaut, W., McFiggans, G., Mentel, Th. F., Monod, A., Prévôt, A. S. H., Seinfeld, J.
677 H., Surratt, J. D., Szmigielski, R., and Wildt, J.: The formation, properties and impact of
678 secondary organic aerosol: current and emerging issues, Atmos. Chem. Phys., 9,
679 5155–5236, doi:10.5194/acp-9-5155-2009, 2009.
680 Harley, R. A., Coulter-Burke, S. C., Yeung, T. S.: Relating liquid fuel and headspace vapor
681 composition for California reformulated gasoline samples containing ethanol, Environ.
682 Sci. Technol., 34, 4088–4094, 2000.
683 Hayes, P. L., Ortega, A. M., Cubison, M. J., Froyd, K. D., Zhao, Y., Cliff, S. S., Hu, W. W.,
684 Toohey, D. W., Flynn, J. H., Lefer, B. L., Grossberg, N., Alvarez, S., Rappengluck, B.,
685 Taylor, J. W., Allan, J. D., Holloway, J. S., Gilman, J. B., Kuster, W. C., de Gouw, J. A.,
686 Massoli, P., Zhang, X., Liu, J., Weber, R. J., Corrigan, A. L., Russell, L. M., Isaacman, G.,
687 Worton, D. R., Kreisberg, N. M., Goldstein, A. H., Thalman, R., Waxman, E. M.,
688 Volkamer, R., Lin, Y. H., Surratt, J. D., Kleindienst, T. E., Offenberg, J. H., Dusanter, S.,
689 Griffith, S., Stevens, P. S., Brioude, J., Angevine, W. M., Jimenez, J. L.: Organic aerosol
690 composition and sources in Pasadena, California during the 2010 CalNex Campaign, J.
691 Geophys. Res.-Atmos., 118, 9233–9257, doi:10.1002/jgrd.50530, 2013.
692 Hou, B., Zhuang, G. S., Zhang, R., Liu, T. N., Guo, Z. G., Chen, Y.: The implication of

carbonaceous aerosol to the formation of haze: Revealed from the characteristics and sources of OC/EC over a mega-city in China, Journal of Hazardous Materials, 190, 529–536, 2011.

Huang, C., Chen, C. H., Li, L., Cheng, Z., Wang, H. L., Huang, H. Y., Streets, D. G., Wang, Y. J., Zhang, G. F., and Chen, Y. R.: Emission inventory of anthropogenic air pollutants and VOC species in the Yangtze River Delta region, China, Atmos. Chem. Phys., 11, 4105–4120, doi:10.5194/acp-11-4105-2011, 2011.

Huang, C., Lou, D. M., Hu, Z. Y., Feng, Q., Chen, Y. R., Chen, C. H., Tan, P. Q., Yao, D.: A PEMS study of the emissions of gaseous pollutants and ultrafine particles from gasoline- and diesel-fueled vehicles, Atmospheric Environment, 77, 703–710, 2013.

Huang, R. J., Zhang, Y. L., Bozzetti, C., Ho, K. F., Cao, J. J., Han, Y. M., Daellenbach, K. R., Slowik, J. G., Platt, S. M., Canonaco, F., Zotter, P., Wolf, R., Pieber, S. M., Bruns, E. A., Crippa, M., Ciarelli, G., Piazzalunga, A., Schwikowski, M., Abbaszade, G., Schnelle-Kreis, J., Zimmermann, R., An, Z., Szidat, S., Baltensperger, U., El Haddad, I., Prévôt, A. S. H.: High secondary aerosol contribution to particulate pollution during haze events in China, Nature, 514, 218–222, doi:10.1038/nature13774, 2014.

Huang, X. F., He, L. Y., Xue, L., Sun, T. L., Zeng, L. W., Gong, Z. H., Hu, M., Zhu, T.: Highly time-resolved chemical characterization of atmospheric fine particles during 2010 Shanghai World Expo, Atmos. Chem. Phys., 12, 4897–4907, doi:10.5194/acp-12-4897-2012, 2012.

Huang, X. F., Xue, L., Tian, X. D., Shao, W. W., Sun, T. L., Gong, Z. H., Ju, W. W., Jiang, B., Hu, M., He, L. Y.: Highly time-resolved carbonaceous aerosol characterization in Yangtze River Delta of China: Composition, mixing state and secondary formation, Atmospheric Environment, 64, 200-207, 2013.

Hung, H. F. and Wang, C. S.: Formation of secondary organic aerosols and reactive oxygen species from diluted motorcycle exhaust, J. Chin. Inst. Chem. Eng., 37, 491−499, 2006.

Huo, H., Yao, Z. L., Zhang, Y. Z., Shen, X. B., Zhang, Q., Ding, Y., He, K. B.: On-board measurements of emissions from light-duty gasoline vehicles in three mega-cities of

China, Atmospheric Environment, 49, 371-377, 2012a.

Huo, H., Yao, Z. L., Zhang, Y. Z., Shen, X. B., Zhang, Q., He, K. B.: On-board measurements of emissions from diesel trucks in five cities in China, Atmospheric Environment, 54, 159-167, 2012b.

Jathar, S. H., Miracolo, M. A., Tkacik, D. S., Donahue, N. M., Adams, P. J., and Robinson, A. L.: Secondary organic aerosol formation from photo-oxidation of unburned fuel: Experimental results and implications for aerosol formation from combustion emissions, Environ. Sci. Technol., 47, 12886−12893, 2013.

Jimenez, J. L.: Ph. D thesis of Understanding and quantifying motor vehicle emissions with vehicle specific power and TILDAS remote sensing, Massachusetts: Massachusetts Institute of Technology, 1999.

Jimenez, J. L., Canagaratna, M. R., Donahue, N. M., Prévôt, A. S. H., Zhang, Q., et al.: Evolution of organic aerosols in the atmosphere, Science, 326 (5959), 1525−1529, 2009.

Kleindienst, T. E., Corse, E.W., Li,W., McIver, C. D., Conver, T. S., Edney, E. O., Driscoll, D. J., Speer, R. E., Weathers, W. S., and Tejada, S. B.: Secondary organic aerosol formation from the irradiation of simulated automobile exhaust, J Air Waste Manage., 52, 259–272, 2002.

Liu, S., Ahlm, L., Day, D. A., Russell, L. M., Zhao, Y. L., Gentner, D. R., Weber, R. J., Goldstein, A. H., Jaoui, M., Offenberg, J. H., Kleindienst, T. E., Rubitschun, C., Surratt, J. D., Sheesley, R. J., and Scheller, S.: Secondary organic aerosol formation from fossil fuel sources contribute majority of summertime organic mass at Bakersfield, J. Geophys. Res.-Atmos., 117, D00V26, doi:10.1029/2012JD018170, 2012

Liu, Y., Shao, M., Fu, L. L., Lu, S.H., Zeng, L. M., Tang, D. G.: Source profiles of volatile organic compounds (VOCs) measured in China: Part I, Atmospheric Environment, 42, 6247–6260, 2008.

May, A.A., Nguyen, N.T., Presto, A.A., Gordon, T.D., Lipsky, E.M., Karve, M., Gutierrez, A., Robertson, W.H., Zhang, M., Brandow, C., Chang, O., Chen, S., Cicero-Fernandez, P., Dinkins, L., Fuentes, M., Huang, S.M., Ling, R., Long, J., Maddox, C., Massetti, J.,

McCauley, E., Miguel, A., Na, K., Ong, R., Pang, Y., Rieger, P., Sax, T., Truong, T., Vo, T., Chattopadhyay, S., Maldonado, H., Maricq, M.M., Robinson, A.L.: Gas- and particle-phase primary emissions from in-use, on-road gasoline and diesel vehicles, Atmospheric Environment, 88, 247–260, 2014.

Na, K., Kim, Y. P., Moon, I., Moon, K. C.: Chemical composition of major VOC emission sources in the Seoul atmosphere, Chemosphere, 55, 585–594, 2004.

Ng, N. L., Kroll, J. H., Chan, A. W. H., Chhabra, P. S., Flagan, R. C., and Seinfeld, J. H.: Secondary organic aerosol formation from m-xylene, toluene, and benzene, Atmos. Chem. Phys., 7, 3909–3922, doi:10.5194/acp-7-3909-2007, 2007.

Nordin, E. Z., Eriksson, A. C., Roldin, P., Nilsson, P. T., Carlsson, J. E., Kajos, M. K., Hellén, H.,Wittbom, C., Rissler, J., Löndahl, J., Swietlicki, E., Svenningsson, B., Bohgard, M., Kulmala, M., Hallquist, M., and Pagels, J. H.: Secondary organic aerosol formation from idling gasoline passenger vehicle emissions investigated in a smog chamber, Atmos. Chem. Phys., 13, 6101–6116, doi:10.5194/acp-13-6101-2013, 2013.

Odum, J. R., Jungkamp, T. P. W., Griffin, R. J., Forstner, H. J. L., Flagan, R. C., and Seinfeld, J. H.: Aromatics, reformulated gasoline, and atmospheric organic aerosol formation, Environ. Sci. Technol., 31, 1890–1897, 1997.

Platt S. M., El Haddad, I., Zardini, A. A., Clairotte, M., Astorga, C., Wolf, R., Slowik, J. G., Temime-Roussel, B., Marchand, N., Ježek, I., Drinovec, L., Močnik, G., Möhler, O., Richter, R., Barmet, P., Bianchi, F., Baltensperger, U., and Prévôt, A. S. H.: Secondary organic aerosol formation from gasoline vehicle emissions in a new mobile environmental reaction chamber, Atmos. Chem. Phys., 13, 9141–9158, doi:10.5194/acp-13-9141-2013, 2013.

Robinson, A. L., Donahue, N. M., Shrivastava, M. K., Weitkamp, E. A., Sage, A. M., Grieshop, A. P., Lane, T. E., Pierce, J. R., and Pandis, S. N.: Rethinking organic aerosols: Semivolatile emissions and photochemical aging, Science, 315, 1259–1262, 2007.

SCCTPI (Shanghai City Comprehensive Transportation Planning Institute): Shanghai comprehensive transportation annual report, Shanghai, 2012.

777 Schauer, J. J., Kleeman, M., Cass, G., Simoneit, B. T.: Measurement of emissions from air
778 pollution sources. 2. C1 through C30 organic compounds from medium duty diesel
779 trucks, Environ. Sci. Technol., 33, 1578–1587, 1999.
780 Schauer, J. J., Kleeman, M., Cass, G., Simoneit, B. T.: Measurement of emissions from air
781 pollution sources. 5. C1-C32 organic compounds from gasoline-powered motor vehicles,
782 Environ. Sci. Technol., 36, 1169–1180, 2002.
783 Stone, E. A., Zhou, J., Snyder, D. C., Rutter, A. P., Mieritz, M., and Schauer, J. J.: A
784 comparison of summertime secondary organic aerosol source contributions at contrasting
785 urban locations, Environ. Sci. Technol., 43, 3448–3454, 2009.
786 Takegawa, N., Miyakawa, T., Kondo, Y., Jimenez, J. L., Zhang, Q., Worsnop, D. R., Fukuda,
787 M.: Seasonal and diurnal variations of submicron organic aerosol in Tokyo observed
788 using the Aerodyne aerosol mass spectrometer, J. Geophys. Res.-Atmos., 111, D11206,
789 doi:10.1029/2005JD006515, 2006.
790 Turpin, B. J. and Lim, H. J.: Species contributions to $PM_{2.5}$ mass concentrations: Revisiting
791 common assumptions for estimating organic mass, Aerosol Science and Technology, 35,
792 602-610, 2001.
793 Wang, H. K., Chen, C. H., Huang, C., Fu, L.X.: On-road vehicle emission inventory and its
794 uncertainty analysis for Shanghai, China. Science of the Total Environment, 398, 60–67,
795 2008.
796 Wang, H. L., Chen, C. H., Wang, Q., Huang, C., Su, L. Y., Huang, H. Y., Lou, S. R., Zhou, M.,
797 Li, L., Qiao, L. P., Wang, Y. H.: Chemical loss of volatile organic compounds and its
798 impact on the source analysis through a two-year continuous measurement, Atmospheric
799 Environment, 80, 488–498, 2013.
800 Wang, J., Jin, L. M., Gao, J. H., Shi, J. W., Zhao, Y. L., Liu, S. X., Jin, T. S., Bai, Z. P., Wu, C.
801 Y.: Investigation of speciated VOC in gasoline vehicular exhaust under ECE and
802 EUDC test cycles, Science of the Total Environment, 445–446, 110–116, 2013.
803 Warneke, C., de Gouw, J. A., Goldan, P. D., Kuster, W. C., Williams, E. J., Lerner, B. M.,
804 Jakoubek, R., Brown, S. S., Stark, H., Aldener, M., Ravishankara, A. R., Roberts, J. M.,

Marchewka, M., Bertman, S., Sueper, D. T., McKeen, S. A., Meagher, J. F., and Fehsenfeld, F. C.: Comparison of daytime and nighttime oxidation of biogenic and anthropogenic VOCs along the New England coast in summer during New England Air Quality Study 2002, J. Geophys. Res.-Atmos., 109, D10309, doi:10.1029/2003jd004424, 2004.

Weitkamp, E. A., Sage, A. M., Pierce, J. R., Donahue, N. M., and Robinson, A. L.: Organic aerosol formation from photochemical oxidation of diesel exhaust in a smog chamber, Environ. Sci. Technol., 41, 6969–6975, 2007.

Wu, Y., Zhang, S. J., Li, M. L., Ge, Y. S., Shu, J. W., Zhou, Y., Xu, Y. Y., Hu, J. N., Liu, H., Fu, L. X., He, K. B., Hao, J. M.: The challenge to NOx emission control for heavy-duty diesel vehicles in China, Atmos. Chem. Phys., 12, 9365–9379, 2012.

Ye, B. M., Ji, X. L., Yang, H. Z., Yao, X. H., Chan, C. K., Cadle, S. H., Chan, T., Mulawa, P. A.: Concentration and chemical composition of $PM_{2.5}$ in Shanghai for a 1-year period, Atmospheric Environment, 37, 499–510, 2003.

Yuan, B., Hu, W. W., Shao, M., Wang, M., Chen, W. T., Lu, S. H., Zeng, L. M., and Hu, M.: VOC emissions, evolutions and contributions to SOA formation at a receptor site in eastern China, Atmos. Chem. Phys., 13, 8815–8832, doi:10.5194/acp-13-8815-2013, 2013.

Zhang, Y. L., Wang, X. M., Zhang, Z., Lü, S. J., Shao, M., Lee, S. C., Yu, J. Z.: Species profiles and normalized reactivity of volatile organic compounds from gasoline evaporation in China, Atmospheric Environment, 79, 110–118, 2013.

Zhao, Y. L., Hennigan, C. J., May, A. A., Tkacik, D. S., de Gouw, J. A., Gilman, J. B., Kuster, W. C., Borbon, A., Robinson, A. L.: Intermediate-volatility organic compounds: a large source of secondary organic aerosol, Environ. Sci. Technol., 48, 13743−13750, 2014.

829

830 **Table 1.** Daily VKT and average speeds of various vehicle and road types in Shanghai in 2012.

Road types	Daily vehicle kilometers traveled (million km)								Average speed ($km \cdot h^{-1}$)
	Light-duty car	Light-duty truck	Taxi	Heavy-duty bus	Heavy-duty truck	City bus	Motor-cycle	Total	
Highway	38.3	0.62	3.96	3.10	11.82	0.23	0.00	58.04	57.9
Arterial road	22.6	2.93	6.16	1.12	4.73	1.58	5.29	44.41	36.0
Residential road	18.3	3.11	8.92	0.89	1.90	1.38	4.15	38.64	28.5
Total	79.2	6.66	19.04	5.11	18.45	3.19	9.44	141.09	43.0

831

832

833 **Table 2.** Test vehicle specifications.

ID	Vehicle type	Fuel type	Emission standard	Model year	Odometer reading (km)
LDGV-1	Light-duty car	Gasoline	Euro 1	2002	245306
LDGV-2	Light-duty car	Gasoline	Euro 2	2005	59790
LDGV-3	Light-duty car	Gasoline	Euro 3	2008	87662
LDGV-4	Light-duty car	Gasoline	Euro 3	2008	80856
Taxi-1	Light-duty taxi	Gasoline	Euro 1	2001	270000
Taxi-2	Light-duty taxi	Gasoline	Euro 1	2002	~100000
Taxi-3	Light-duty taxi	Gasoline	Euro 2	2003	99638
Taxi-4	Light-duty taxi	Gasoline	Euro 3	2007	281315
Taxi-5	Light-duty taxi	Gasoline	Euro 3	2008	361180
HDDT-1	Heavy-duty truck	Diesel	Euro 1	2003	331387
HDDT-2	Heavy-duty truck	Diesel	Euro 1	2003	271000
HDDT-3	Heavy-duty truck	Diesel	Euro 2	2004	271125
HDDT-4	Heavy-duty truck	Diesel	Euro 2	2004	204193
HDDT-5	Heavy-duty truck	Diesel	Euro 3	2009	70000
Bus-1	City bus	Diesel	Euro 2	2006	295236
Bus-2	City bus	Diesel	Euro 3	2006	175122
MT-1	Motorcycle	Gasoline	Euro 1	2003	15000
MT-2	Motorcycle	Gasoline	Euro 1	2003	11191
MT-3	Motorcycle	Gasoline	Euro 2	2004	96969
MT-4	Motorcycle	Gasoline	Euro 2	2003	13912
MT-5	Motorcycle	Gasoline	Euro 2	2003	5379

834

835

836

837

838 **Table 3.** Vehicle emission inventory in Shanghai.

Vehicle type	Emission inventory (k ton)					
	CO	NOx	VOCs	EVA	EC	POA (OC*1.2)
in vehicle type						
LDGV	192.03	13.30	15.59	6.15	0.02	0.07
LDDV	1.89	5.72	0.32	0.00	0.17	0.11
Taxi	68.89	3.86	5.56	1.96	0.01	0.03
HDGV	36.79	2.20	2.29	0.29	0.00	0.01
HDDV	24.71	67.56	9.74	0.00	3.16	3.40
Bus	5.53	17.56	2.06	0.00	0.58	0.62
Motorcycle	14.01	0.67	3.85	0.49	0.02	0.06
in fuel type						
Gasoline	311.71	20.04	27.28	8.88	0.05	0.17
Diesel	32.14	90.84	12.12	0.00	3.91	4.13
Total	343.85	110.88	39.40	8.88	3.96	4.30

839

840

841

842

843

844

845

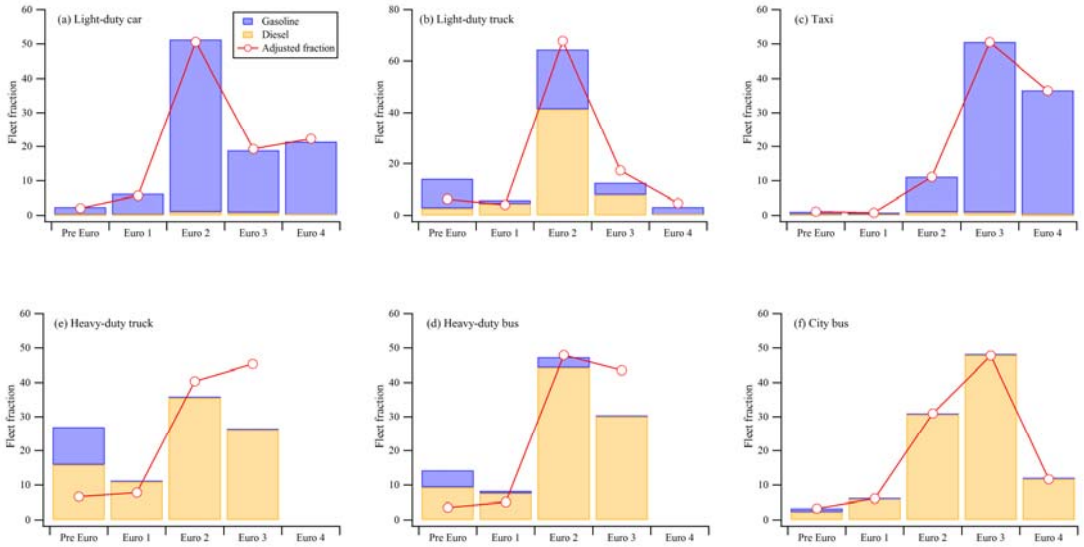

Fig. 1. Static and adjusted fractions of each vehicle type in Shanghai.

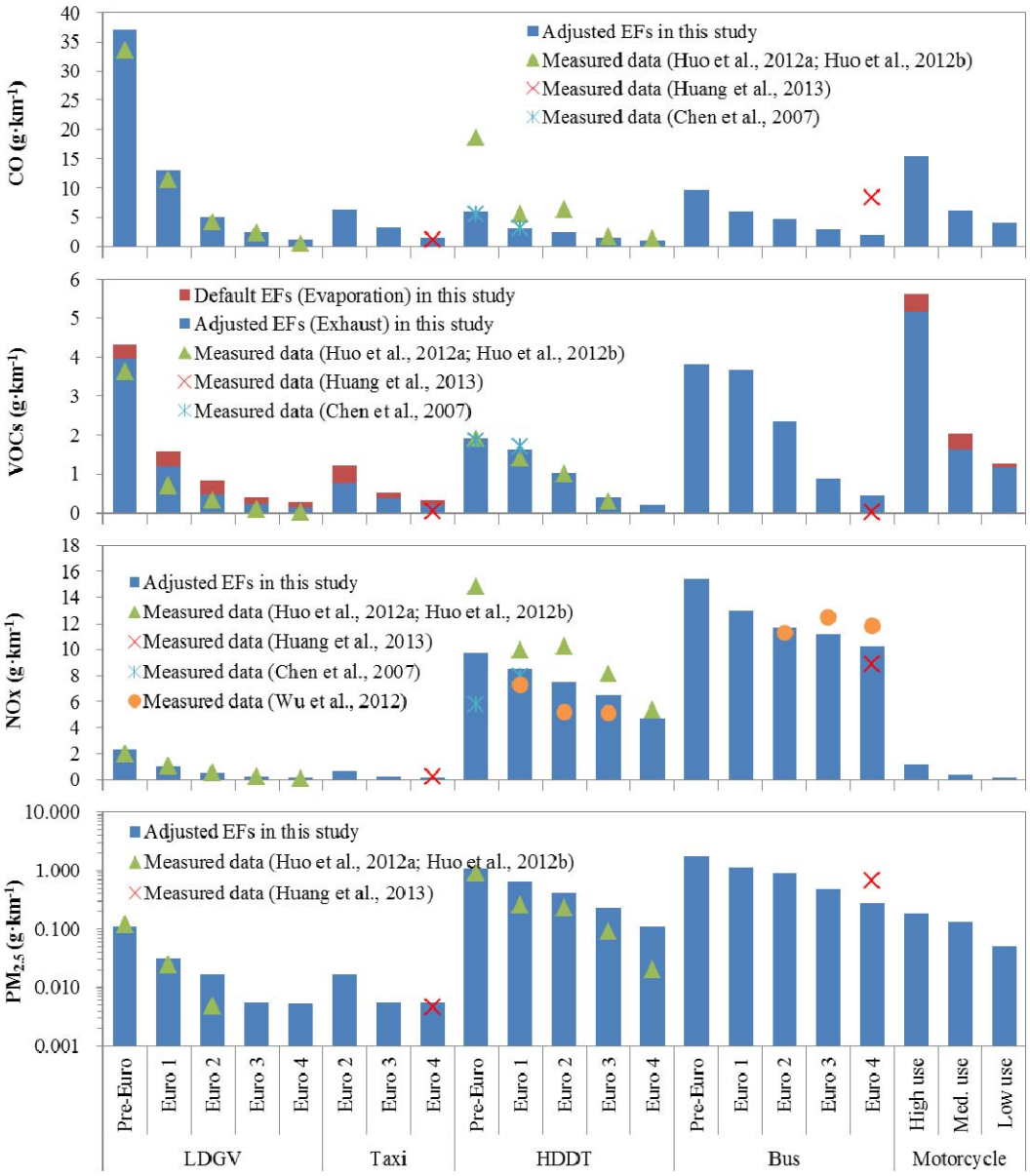

Fig. 2. Adjusted emission factors of various vehicle types (blue bars) and their comparisons with measured emission factors in the previous studies (dots).

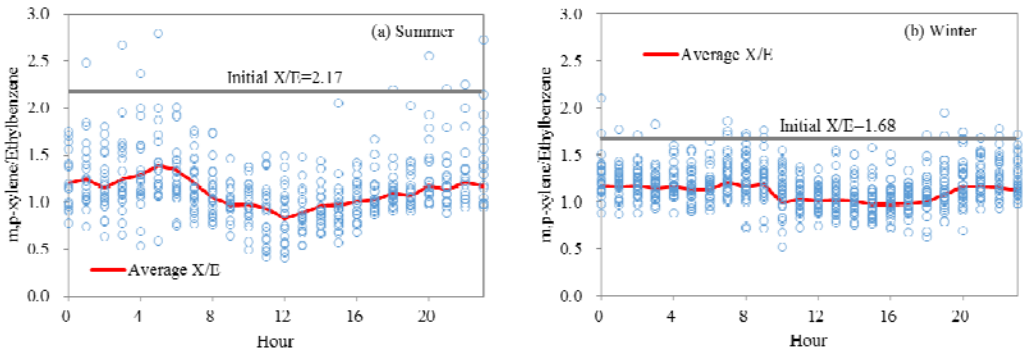

Fig. 3. Diurnal distributions of the ratios of m,p-xylene to ethylbenzene concentrations in summer and winter in the urban atmosphere in 2013.

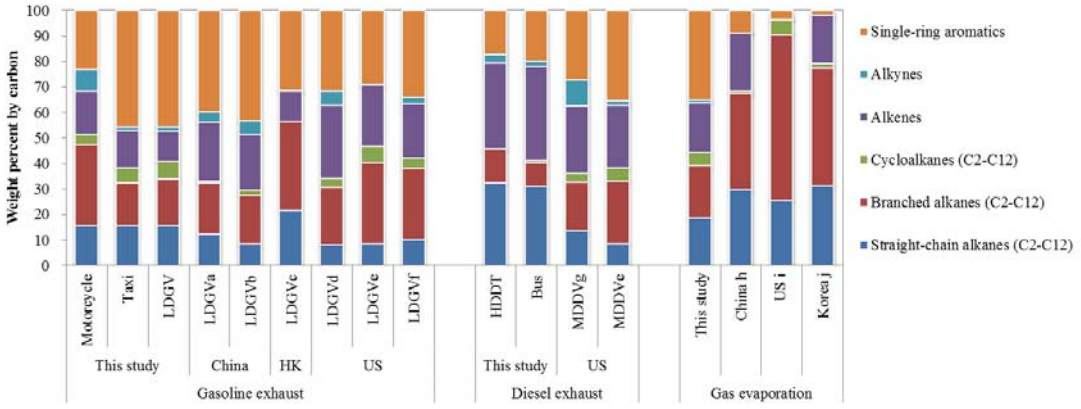

Fig. 4. Comparisons of measured VOC compositions of the exhausts from different vehicle types and gas evaporation to the results in other studies (a. Liu et al., 2008; b. Wang et al., 2013; c. Guo et al., 2011; d. Schauer et al., 2002; e. May et al., 2014; f. Gentner et al., 2013; g. Schauer et al., 1999; h. Zhang et al., 2013; i. Harley et al., 2000; j. Na et al., 2004).

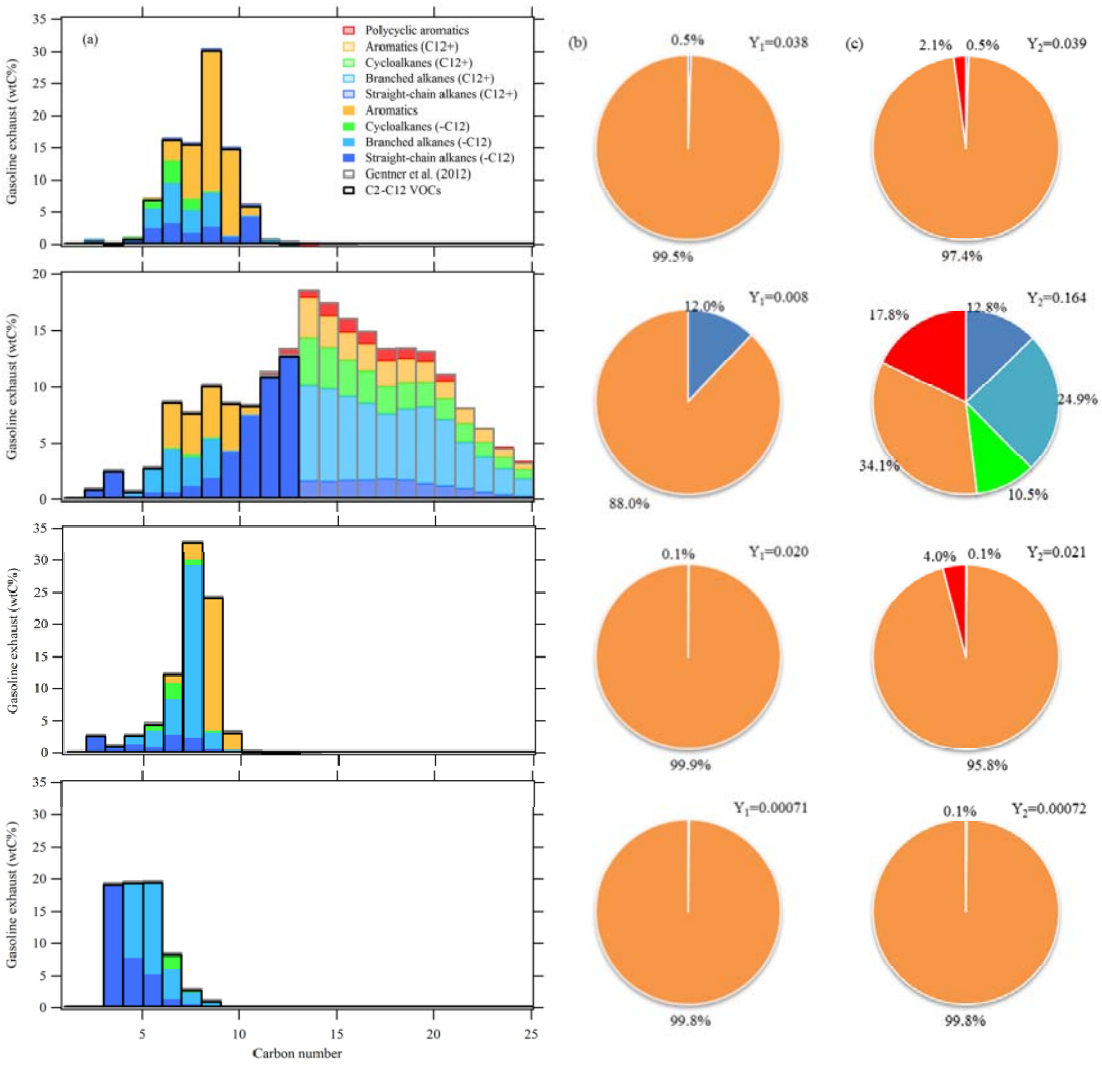

873

874 **Fig. 5.** (a) Distribution of mass by chemical class in carbon number of different vehicle exhausts
875 and evaporative emissions; (b) Calculated SOA yields based on C2-C12 VOCs measured in this
876 study and their contributors; (c) Calculated SOA yields based on C2-C25 VOCs combined with
877 S/IVOC species in unburned fuel referenced from Gentner et al. (2012) and their contributors.

878

879

880

881

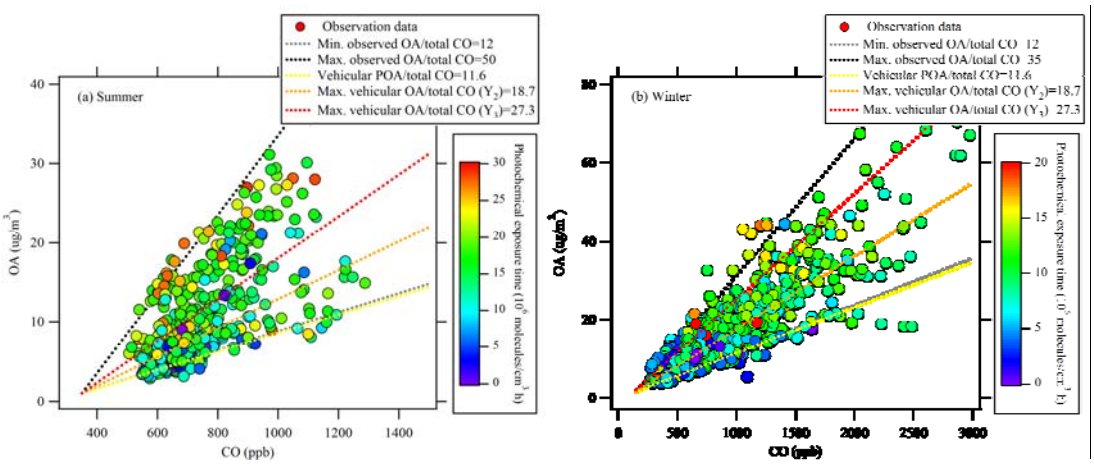

Fig. 6. Relationship of measured OA and CO concentrations color-coded by the photochemical exposure in the summer (a) and winter (b) of 2013 in urban Shanghai according to equation (4). Minimum and maximum ratios of observed OA to CO concentrations are shown by dotted grey and black lines. Vehicular POA/Total CO is shown by dotted yellow line. The minimum and maximum OA formation ratios of vehicle emissions calculated with two different SOA yields of Y2 and Y3 are shown by the dotted orange and red lines, respectively.

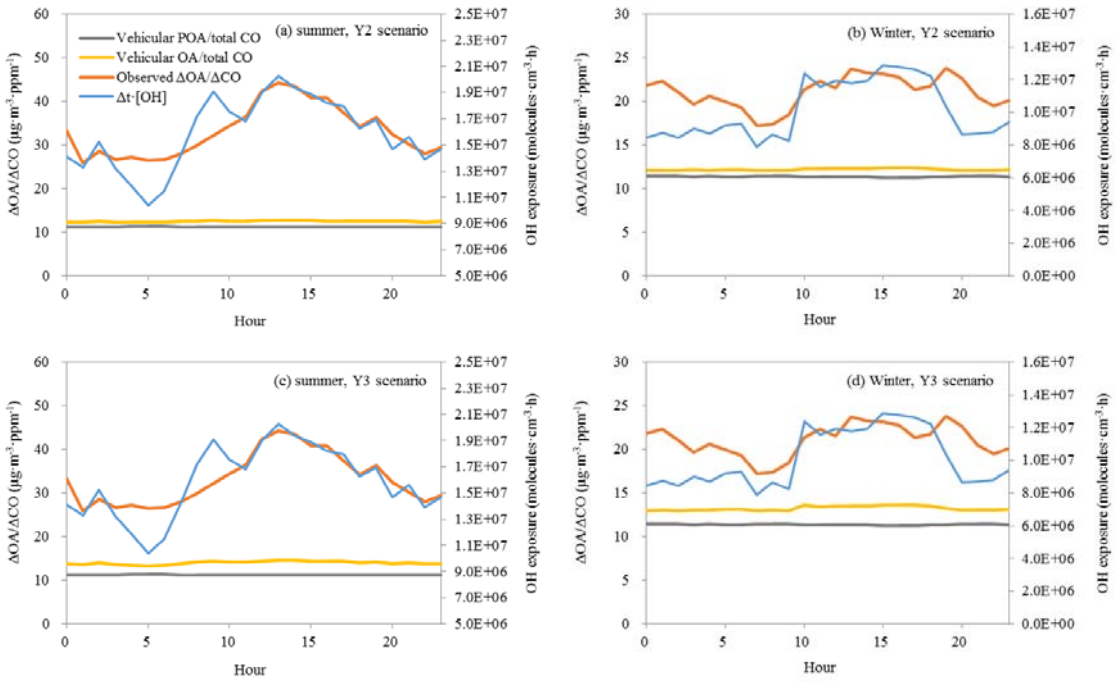

Fig. 7. Diurnal variations of observed ΔOA/ΔCO in the atmosphere (red line), OH exposures (blue line), and the ratios of vehicular POA emission (grey line) and OA formation (orange line) to total CO emissionswith the SOA yields in two scenarios (Y2 and Y3) in summer and winter in the urban area of Shanghai for the year of 2013.

916

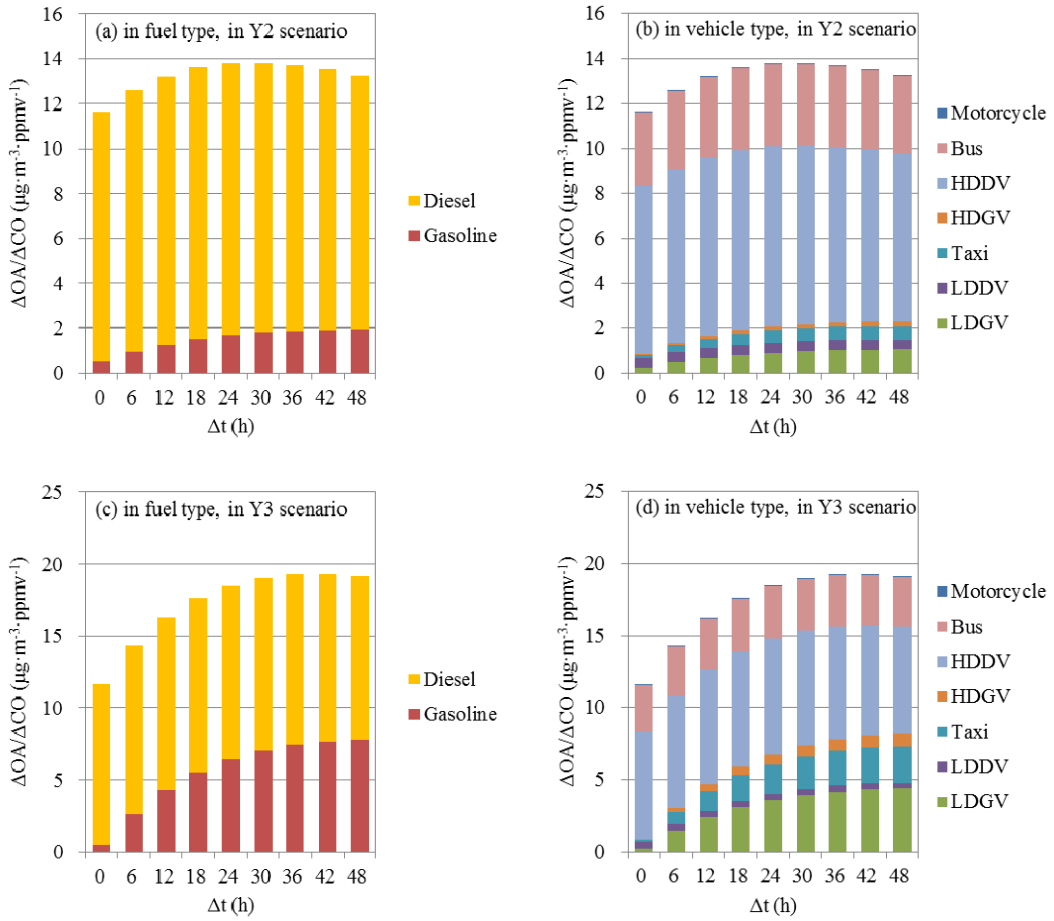

917

918 **Fig. 8.** Contributions of vehicle emissions to OA formation ratios in different vehicle and fuel

919 types in Y2 and Y3 scenarios with the changes of photochemical ages.

920

921